Earth Planets Space, **53**, 611–614, 2001

Global destabilization due to localized reconnection: A mechanism for coronal mass ejections

P. F. Chen[1,2], K. Shibata[2], and T. Yokoyama[3]

[1]*Department of Astronomy, Nanjing University, Nanjing 210093, China,*
[2]*Kwasan Observatory, Kyoto University, Kyoto 607-8471, Japan*
[3]*Nobeyama Radio Observatory, National Astronomical Observatory, Japan*

(Received June 19, 2000; Revised November 27, 2000; Accepted February 20, 2001)

Solar CMEs are large scale eruptive phenomena, while flux emergence is a local event on the Sun. Our numerical simulations show that two categories of reconnection-favored emerging flux can trigger the destabilization and the ejection of the filament (i.e., CME): within the filament channel or on the outer edge of the channel, which confirms recent important observations by Feynman and Martin (1995). In particular for the latter category, numerical results show that there is a critical amount for the emerging flux, below which the flux rope eruption cannot be triggered. Our numerical model, for the first time, provides a physical explanation for the observed correlation between CMEs and the reconnection-favored emerging flux.

1. Introduction

Since their identification in early 1970s, coronal mass ejections (CMEs) have attracted a lot of interest by their own extreme characteristics (e.g., large scale, etc.), as well as their relation with other solar activities and geomagnetic activities. The most interesting aspect is that of their origin (Hundhausen, 1999).

CMEs represent a type of global magnetic changes, and many models have been proposed for their onset mechanism. Magnetic arcades with shear motion are widely studied. It is found that there exists a critical shear amount, beyond which even a little more shear can make the closed magnetic arcades asymptotically approach the open field, while resistive instability can result in the eruption (cf. Mikić and Linker, 1994 and references therein). However, for the pure shear motion, it may take an unrealistically long time for the shear to exceed the critical value. Converging motion of the magnetic arcades can also lead to the destabilization of the filament structure (Inhester *et al.*, 1992; Forbes and Priest, 1995). This can be easily understood as the increase of the magnetic pressure near the solar surface. Recently, Wu and Guo (1997) simulated the emerging processes of magnetic bubble. They show that the emerging magnetic bubble, if it is strong enough, can destabilize helmet streamers to form CMEs.

Flux emergence is a kind of small scale event, which can produce flares (Shibata *et al.*, 1992; Yokoyama and Shibata, 1996). Statistical study by Feynman and Martin (1995) shows that many CMEs are correlated to localized emerging flux. Their research also indicates that the emerging flux favorable for magnetic reconnection with pre-existing field has a very high probability of triggering filament eruptions (and CMEs). Based on numerical simulations, we have proposed an emerging flux trigger mechanism for CMEs, which provides a physical explanation for the observed correlation between CMEs and the reconnection-favored emerging flux (Chen and Shibata, 2000). This paper further studies the parameter-dependency in the model.

2. Numerical Method

Two-dimensional time dependent compressible resistive MHD equations are numerically solved by a multistep implicit scheme (see Hu, 1989; Chen *et al.*, 1999 for details). The five independent variables are density (ρ), velocity (v_x, v_y), magnetic flux function (ψ), and temperature (T). The characteristic values for ρ, T are $\rho_0 = 1.67 \times 10^{-12}$ kg m^{-3}, $T_0 = 10^6$ K, respectively. Plasma β (the ratio of gas to magnetic pressure) is chosen to be 0.01, a typical value for the solar corona, so that the corresponding Alfv́en speed v_A is 1818 km s^{-1}. Heat conduction and gravity are omitted here, and therefore the dimensionless results are independent of the length scale, L_0, as indicated by Chen *et al.* (1999). Here, we might as well consider $L_0 = 10^5$ km, and so the Alfv́en transit time τ_A equals 55 s. The resistivity η has the following current-density dependent form:

$$\eta/(\mu_0 v_0 L_0) = \begin{cases} \eta_0 \min\left(1, \left|\dfrac{j_z}{j_c}\right| - 1\right), & |j_z| \geq j_c; \\ 0, & |j_z| < j_c, \end{cases} \quad (1)$$

where $\eta_0 = 0.02$, j_z is the current density, $j_c = 0.5$ is the critical value of j_z, beyond which the resistivity is assumed to be excited. It was suggested that the current dependent resistivity model as Eq. (1) can lead to fast reconnection (Tajima and Shibata, 1997).

To account for the observational features of many filaments, such as the inverse polarity and the cavity structure, a

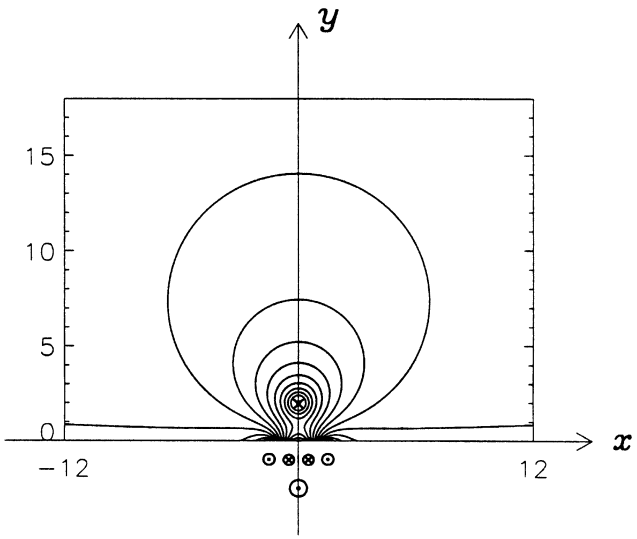

Fig. 1. Initial magnetic configuration and its source currents.

flux rope model was put forward for constructing filaments (Kuperus and Raadu, 1974; Chen and Garren, 1993; Low and Smith, 1993). Therefore, our initial magnetic structure is chosen as a flux rope-like configuration as shown in Fig. 1. The magnetic flux function (ψ) is expressed as $\psi = \psi_b + \psi_l - \frac{r_0}{2}\ln(x^2 + (y+h)^2)$, where

$$\psi_b = c \ln \frac{[(x+0.3)^2 + (y+0.3)^2][(x-0.3)^2 + (y+0.3)^2]}{[(x+1.5)^2 + (y+0.3)^2][(x-1.5)^2 + (y+0.3)^2]}, \tag{2}$$

$$\psi_l = \begin{cases} r^2/(2r_0), & r \le r_0; \\ r_0/2 - r_0 \ln(r_0) + r_0 \ln(r), & r > r_0, \end{cases} \tag{3}$$

and $r = \sqrt{x^2 + (y-h)^2}$; $h = 2$; $r_0 = 0.5$.

Uniform temperature $T = T_0$ is assumed. Initial density is distributed as

$$\rho/\rho_0 = \begin{cases} 1 + \frac{2}{\beta}\left(1 - \frac{r^2}{r_0^2}\right), & r \le r_0; \\ 1, & r > r_0. \end{cases} \tag{4}$$

The dimensionless size of the simulation box is $-12 \ge x \ge 12$ and $0 \ge y \ge 18$. The domain is discretized by 161×181 grid points, which are uniformly distributed in the y-direction and nonuniformly along the x-direction.

According to the observational results by Feynman and Martin (1995), two types of reconnection-favored emerging flux can trigger CMEs, i.e., within the filament channel and on the outer edge of the channel, as shown in Fig. 2 and illustrated in Fig. 3. Correspondingly, two cases (A and B) are investigated here: in case A, the flux emergence appears near the magnetic neutral line $x = 0$, and in case B, it appears on the outer edge of the filament channel. To simulate the flux emergence, we change the value of ψ until $t = t_e = 200\ \tau_A$, i.e., $\psi(x, 0, t) = \psi(x, 0, 0) + \psi_e t/t_e$ ($t \le t_e$), in the local region $|x - x_0| \le 0.3$, where ψ_e equals 10 for case A and -10 for case B, x_0 represents the location of the emerging flux. After $t = t_e$, the bottom boundary is fixed.

Note that in Eq. (2), the coefficient c is determined by trial and error in order to guarantee that the flux rope center approximately keeps stable for long enough time. In our simulations, c is set to be 2.5628.

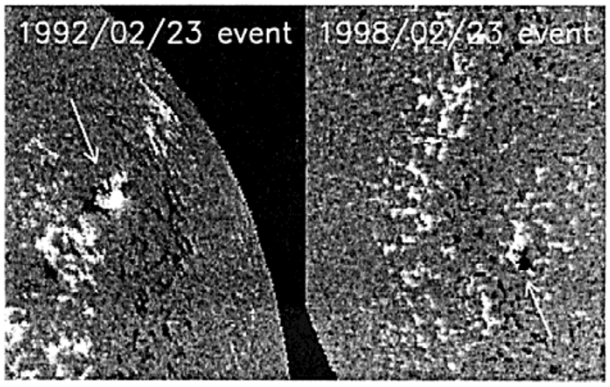

Fig. 2. Two categories of reconnection-favored emerging flux: within the filament channel (left panel) and on the outer edge of the filament channel (right panel).

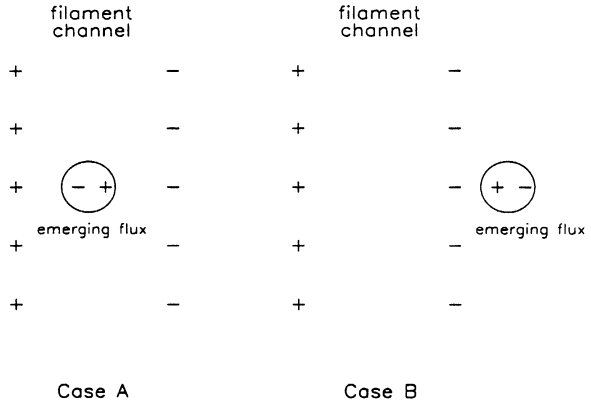

Fig. 3. Sketch map of the two categories of reconnection-favored emerging flux. Case A: within the filament channel; Case B: on the outer edge of the channel.

3. Numerical Results

In case A, the emerging flux appears near the neutral line, i.e., $|x| \le 0.3$, with direction opposite to the ambient coronal field. Magnetic reconnection occurs as the new flux emerges, which leads to partial magnetic cancellation, and therefore the decrease of magnetic pressure. The magnetized plasma at both sides (left and right to the null point) is seen to move inwardly as illustrated in the upper panel of Fig. 4. As the frozen-in field lines accumulate near the y-axis, the current density (j_z) near the neutral line increases nearly exponentially with time until $t = 65\ \tau_A$. As j_z exceeds j_c, resistivity is excited, fast reconnection occurs at an X-point. As shown in the upper panel of Fig. 5, the plasma above the X-point is accelerated by the magnetic tension of the reconnected field lines. The resulting upward jet collides with the flux rope to form an upward-propagating reverse fast shock, by which the flux rope is pushed away until it moves out of the top boundary. Below the X-point, the reconnection outflow collides with the line-tied magnetic loops, and a cusp-shaped structure with high temperature is clearly seen, which is the

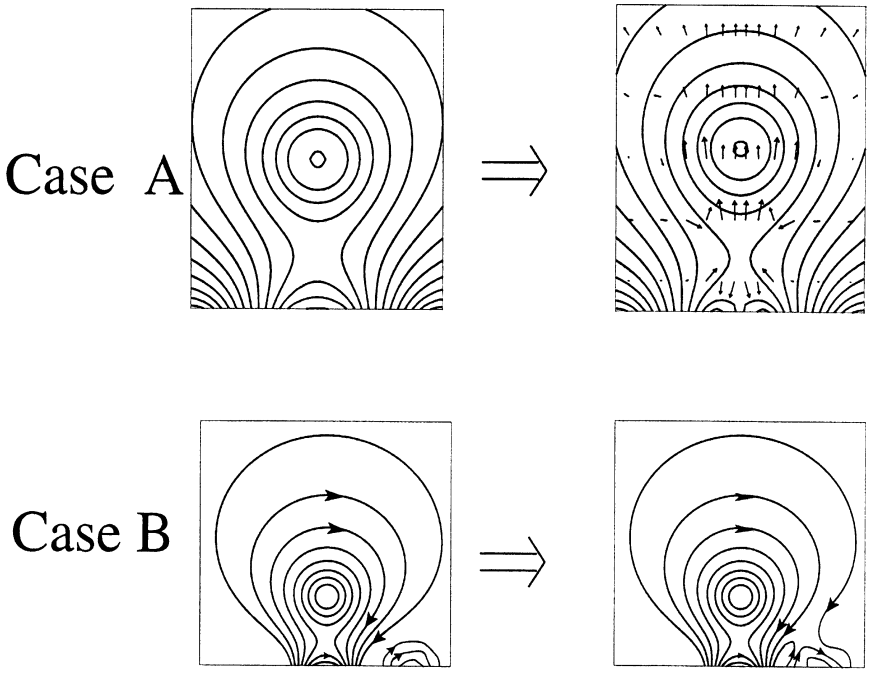

Fig. 4. Sketch map of the triggering processes in the two cases.

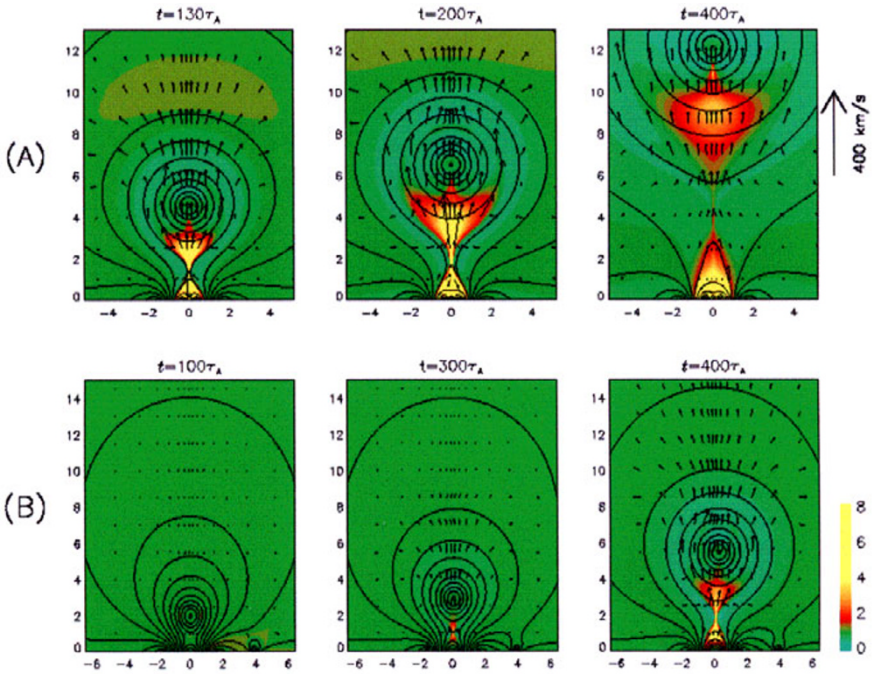

Fig. 5. MHD evolution in case A (upper panel) and case B (lower panel). Solid lines correspond to the magnetic field, arrows to the velocity, and the color map to the temperature.

typical soft X-ray feature of LDE (long duration event) flares, as numerically simulated in detail by Chen *et al*. (1999).

In case B, the emerging flux is introduced within $|x - 3.9| \leq 0.3$ at the bottom. As illustrated in the lower panel of Fig. 4, reconnection between the emerging flux and the coronal field rearranges the magnetic configuration. The reconnected field lines, which are firstly connected to the left-hand side of the emerging region, are diverted to its right-hand side, and are ejected outward along with reconnection outflow. The flux rope follows the reconnection inflow to move upward, and then, the local region below the flux rope becomes evacuated, so that magnetized plasma at both sides (left and right to the null point) is driven by the gradient total pressure to move inwardly. Similar to case A, a current sheet is formed below the flux rope. As the current density exceeds the critical value, resistivity is excited, and the following

reconnection and flux rope eruption processes are similar to case A, as indicated by the lower panel of Fig. 5.

4. Discussions

As suggested by observations (Feynman and Martin, 1995), two types of emerging flux with reconnection-favored direction can trigger filament eruptions (and then CMEs): one is within the filament channel, the other is on the outer edge of the channel. Our two cases (A and B) correspond to these two categories, respectively. In case A, the emerging flux reconnects with the magnetic loops below the flux rope, and leads to partial magnetic cancellation, which decreases the local magnetic pressure. Then, the magnetized plasma at the two sides is pressed by the resulting magnetic pressure gradient to move inwardly, and the frozen-in field lines accumulate near the y-axis to form a current sheet. Meanwhile, the flux rope loses its equilibrium, and moves upward. In case B, the emerging flux reconnects with the overlying magnetic field of the flux rope. After reconnection, the two laterally interacting magnetic loops evolve to a small inner loop and a large outer loop. The locally concave outer loop is ejected outward along with the reconnection outflow. This expansion can also be understood as the decrease of the magnetic tension of the field lines, which become less bent after reconnection. The flux rope is, therefore, accelerated upward. Below the flux rope, plasma moves inwardly, and field lines move along with the inflow and accumulate near the y-axis, then a current sheet is formed below the flux rope.

Such a newly-formed current sheet attracts the flux rope and stops it from continual motion until the flux rope reaches new equilibrium. However, when the current density surpasses a critical value, resistivity is supposed to be excited. The current is then dissipated, and our numerical simulations show a rapid ejection of the flux rope. Below the current sheet, a cusp structure is formed with high temperature, which is considered as the signature of solar flares or arcades in soft X-ray (SXR).

Further simulations indicate that when reconnection-favored flux emerges within the filament channel as case A, however tiny it may be, it can trigger the upward motion of the flux rope (note here that the upward motion does not mean an eruption, which further depends on the occurrence of resistivity in the newly-formed current sheet). On the contrary, when reconnection-favored flux appears on the outer edge of the filament channel as case B, only strong enough emerging flux can trigger the upward motion of the flux rope, i.e., there exists a threshold. As far as the flux emergence is located within $|x - 3.9| \leq 0.3$, the critical flux is $\psi_e \sim -7$, which is comparable with the initial magnetic flux. This result is in agreement with the observation by Feynman and Martin (1995). At the same time, for certain emerging flux, such as $\psi_e = -10$, the emergence location (represented by x_0) should not be too close to the filament channel. When $x_0 < 1.5$, the reconnection-favored emerging flux attracts the flux rope to move down.

It has been observed that weak SXR activity often precedes the flash phase of solar flares (Datlowe *et al.*, 1974) or the linearly extrapolated starting time of the CMEs (Harrison *et al.*, 1985). The localized heating due to the reconnection between the emerging flux and the overlying magnetic field in our numerical results may account for the weak SXR activity, i.e., precursor.

5. Conclusion

Observations show that CMEs are strongly correlated to two categories of reconnection-favored emerging flux (Feynman and Martin, 1995), i.e., within the filament channel or on the outer edge of the channel. To account for the correlation, an emerging flux trigger mechanism is proposed based on the erupting flux rope model for CMEs:

(1) Numerical simulations reproduce the observed correlation between CMEs and reconnection-favored emerging flux, and provide a physical explanation for it, i.e., localized reconnection rearranges the magnetic structure, and triggers the rise motion of the flux rope due to loss of equilibrium. The ensuing reconnection induces the large-scale eruption.

(2) For flux emergence on the outer edge of the filament channel, the above trigger effect depends on the amount and the location of the emerging flux, i.e., the emerging flux should not be too weak and too close to one single polarity of the filament.

Acknowledgments. One of the authors (PFC) thanks all the colleagues at Kwasan Observatory for their hospitality during his stay. He is also supported in part by key projects (No. 4990451 and 19973009) from the National Natural Science Foundation of China.

References

Chen, J. and D. A. Garren, Interplanetary magnetic clouds: Topology and driving mechanism, *Geophys. Res. Lett.*, **20**, 2319–2322, 1993.

Chen, P. F. and K. Shibata, An emerging flux trigger mechanism for coronal mass ejections, *ApJ*, **545**, 524–531, 2000.

Chen, P. F., C. Fang, M. D. Ding, and Y. H. Tang, Flaring loop motion and a unified model for solar flares, *ApJ*, **520**, 853–858, 1999.

Datlowe, D. W., M. J. Elcan, and H. S. Hudson, OSO-7 observations of solar X-rays in the energy range 10–100 keV, *Solar Phys.*, **39**, 155–174, 1974.

Feynman, J. and S. F. Martin, The initiation of coronal mass ejections by newly emerging magnetic flux, *JGR*, **100**, 3355–3367, 1995.

Forbes, T. G. and E. R. Priest, Photospheric magnetic field evolution and eruptive flares, *ApJ*, **446**, 377–389, 1995.

Harrison, R. A., P. W. Waggett, R. D. Bentley, K. J. H. Phillips, M. Bruner, M. Dryer, and G. M. Simnett, The X-ray signature of solar coronal mass, *Solar Phys.*, **97**, 387–400, 1985.

Hu, Y. Q., A multistep implicit scheme for time-dependent 2-dimensional MHD flows, *J. Comput. Phys.*, **84**, 441–460, 1989.

Hundhausen, A., *The Many Faces of the Sun*, edited by K. Strong, J. Saba, B. Haisch, and J. Schmelz, Berlin, Springer, pp. 143–200, 1999.

Inhester, B., J. Birn, and M. Hesse, The evolution of line-tied coronal arcades including a converging footpoint motion, *Solar Phys.*, **138**, 257–281, 1992.

Kuperus, M. and M. A. Raadu, The support of prominences formed in neutral sheets, *A&A*, **31**, 189–193, 1974.

Low, B. C. and D. F. Smith, The free energies of partially open coronal magnetic fields, *ApJ*, **410**, 412–425, 1993.

Mikić, Z. and J. A. Linker, Disruption of coronal magnetic field arcades, *ApJ*, **430**, 898–912, 1994.

Shibata, K., S. Nozawa, and R. Matsumoto, Magnetic reconnection associated with emerging magnetic flux, *PASJ*, **44**, 265–272, 1992.

Tajima, T. and K. Shibata, *Plasma Astrophysics, Addison-Wesley*, 1997.

Wu, S. T. and W. P. Guo, *Coronal Mass Ejections: Geophysical Monogr. 99*, edited by N. Crooker, J. A. Joselyn, and J. Feynman, pp. 83–89, AGU, Washington, D.C., 1997.

Yokoyama, T. and K. Shibata, Numerical simulation of solar coronal X-ray jets based on the magnetic reconnection model, *PASJ*, **48**, 353–376, 1996.

P. F. Chen (e-mail: chenpf@nju.edu.cn), K. Shibata (e-mail: shibata@kwasan.kyoto-u.ac.jp), and T. Yokoyama (e-mail: yokoyama@nro.nao.ac.jp)